DIGITAL REDESIGN OF CONTINUOUS-TIME SYSTEMS WITH THE MODULATED SINE BLOCK-PULSE FUNCTION METHOD

連續時間系統利用調變正弦方塊脈波函數之數位重設計

Fu-Hwa Liu¹, Long-Life Show¹, Lih-Feng Lin¹, Ching-Long Chyr² 柳復華¹,壽鶴年¹,林麗鳳¹,池慶龍²

¹ Department of Aviation & Communication Electronics, Air Force Institute of Technology.

² Department of Computer & Communication, SHU-TE University.

1空軍航空技術學院航空通訊電子系

2樹德科技大學電腦通訊系

Abstract

This study present a new digital redesign method for implemented analog system in which the controller is composed of the forward and feedback gain matrices. Since the design of the proposed method is according to the characteristic of response curve of stable controlled systems, it is more effective for certain digitally redesigned systems. In the proposed method, there is a modulated parameter which can be adjusted in accordance with different system models. When a suitable modulated parameter value in the proposed method is utilized to digitalize an analogue controlled system, the states responses of the new digitally redesigned system are able to closely match those of the original analogous controlled system, and also can tolerate a larger sampling period for sample-data implementation. Thus, the proposed method is more advantageous to the cases in which the sampling rates are relatively slow due to the hardware constraints or to where the transient responses are especially emphasized. A simulated example is used to demonstrate the results.

Keywords: digital redesign, modulated parameter, sampling period.

摘要

這篇論文針對一已完成設計的類比系統,其控制器是由順向及回饋增益矩陣所構成,提出了一種新的數位重設計的方法。因為所提之方法是擷用系統響應曲線之特性,所以在數位重設計系統時將顯得更為有效。在所提方法中有一調變的參數,其可根據不同的系統模型來作調整。當一適當的調變參數值被使用於所提之方法中去數位化一類比受控系統時,其數位化後的響應不僅與原始的類比系統的響應能夠很貼近,且可容忍以相對較大的取樣週期去完成連續資料的被取樣。所提之數位化

重設計方法對於因硬體限制導致慢取樣率的系統或是特別強調暫態反應的系統顯得 更為有用。一個實例將被模擬去驗證這些結果。

關鍵詞:數位化重設計、調變參數、取樣週期。

1. Introduction

Owing to the low cost and high performance of digital technology, a system via digital control is superior to an analog one [1,2]. The digital control has the attractive advantages of flexibility and realization, thus it can tune controller just by reprogramming the control algorithm for further application. Under the influence of unavoidable disturbance or noise, the analog controller needs an additional compensator to eliminate noise, whereas the digital control does not require any hardware extension to form a high-order controller, thus, it can decrease the system complexity. There are two approaches to design a digital control system. The first approach is to design an analogy controller and then redesign it via some discretization methods [3-5]. The second approach is to discretize the controlled plant and then do a discretetime controller. Because most of the real controllers are designed on continuoustime model, for which many theories and practical methods have been developed, so the first redesigned approach is popular and is often used in industry. A continuous-time implemented system is usually designed upon some specific goals, so every redesigned discrete counterpart should match the original one as closely as possible. That is the focus of this paper. For stable continuous-time systems, the system responses frequently resemble the shrinkage of a sine function curve. It is believed that the accordant sine curve response may match well system response. Thus, a modulated sine block-pulse function approximation method is used on the available sampled data in a system response.

The materials in this paper are organized as follows: In the following section, the redesign is briefly discussed. Next, the modulated sine block-pulse function approximation method is presented for the redesign controller. Then, a simulation example is performed to demonstrate the effectiveness of the proposed method, and the results are summarized.

2. Digital redesign

Let us consider the open-loop linear controllable continuous-time system described by

 $\dot{x}_c(t) = Ax_c(t) + Bu_c(t)$, $x_c(0) = x_0$ (1) where $x_c(t)$ and $u_c(t)$ are the $m \times 1$ state vector and the $p \times 1$ input vector, respectively, and A and B are constant matrices of appropriate dimensions. Also, let the continuous-time state-feedback control law in (1) be

$$u_c(t) = -K_c x_c(t) + E_c r(t)$$
 (2)
where $r(t)$ is a reference input with
dimension of $q \times 1$, and the feedback gain
 K_c of dimension $p \times m$ and forward gain
 E_c of dimension $p \times q$ are given. By using
this controller, the designed closed-loop
system becomes

$$\dot{x}_c(t) = \hat{A}x_c(t) + BE_c r(t). \tag{3}$$

representation of (3) is shown in figure 1a.

where $\hat{A} \equiv A - BK_c$. The block diagram

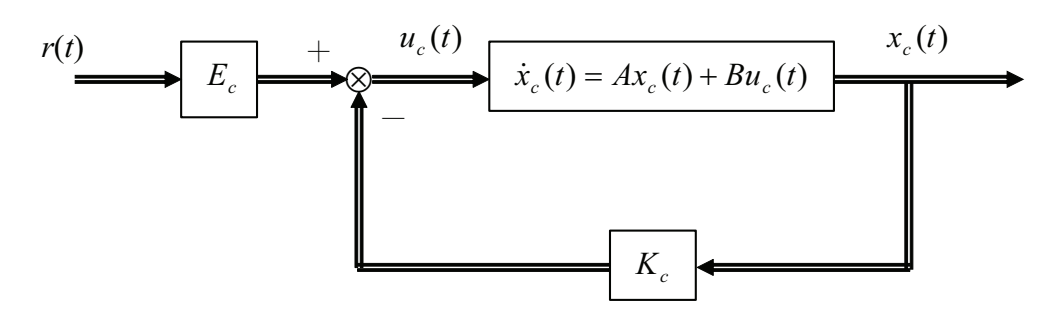


Figure 1a Continuous-time system

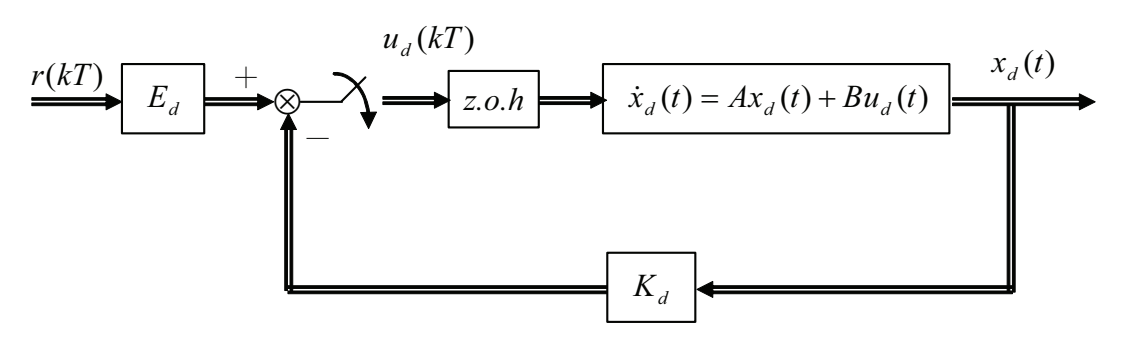


Figure 1b. Redesigned digital system

Let the state equation of the digital system which approximates the continuous-time system in (1) be represented by

$$\dot{x}_d(t) = Ax_d(t) + Bu_d(t), x_d(0) = x_0$$
 (4a)

where $u_d(t)$ is a piecewise-constant input function

$$u_d(t) = u_d(kT)$$
, for $kT \le t < (k+1)T$ (4b)

and T is the sampling period. Let the discrete-time state-feedback control law for the open-loop system in (4) be.

$$u_d(kT) = -K_d x_d(kT) + E_d r(kT). (5)$$

The designed closed-loop system in (4) with the controller in (5) becomes

$$\dot{x}_{d}(t) = Ax_{d}(t) - BK_{d}x_{d}(kT) + BE_{d}r(kT),$$

$$x_{d}(0) = x_{0}.$$
(6)

for $kT \le t < (k+1)T$, where $K_d \in R^{p \times m}$ and $E_d \in R^{p \times q}$ are the digital state-feedback and forward gains, respectively. The block diagram representation of (6) is shown in figure 1b. A zero-order hold is utilized in (3) so that $r(t) \approx r(kT)$ over one sampling

period. Then, the corresponding discretetime models of (3) and (6) can be written as

$$x_{c}(kT+T) = \hat{G}x_{c}(kT) + \hat{H}E_{c}r(kT), \quad x_{c}(0) = x_{0}$$
(7)

and

$$x_d(kT + T) = (G - H K_d)x_d(kT) + HE_d r(kT)$$

 $x_d(0) = x_0$ (8)

respectively, where

$$\hat{G} = \exp\{(A - BK_c)T\}$$
 (9a)

$$\hat{H} = \int_{0}^{T} \exp\{(A - BK_{c})\lambda\} B d\lambda = (\hat{G} - I_{m})(A - BK_{c})^{-1}B$$
(9b)

$$G = \exp(AT), \tag{9c}$$

$$H = \int_0^T \exp(A\lambda)B \, d\lambda = (G - I_m)A^{-1}B, \qquad (9d)$$

Note that if $A - BK_c$ or A is singular, the

computation of \hat{H} or H can be carried out by the use of numerical algorithms [6].

To match all m states $x_d(t)$ in (8) with $x_c(t)$ in (7) at each sampling instant, it is required that

$$\hat{G} = G - HK_{d}, \tag{10a}$$

$$\stackrel{\wedge}{HE}_{a} = HE_{J}, \tag{10b}$$

where the $p \times m$ feedback gain K_d and $p \times q$ forward gain E_d are unknown matrices to be solved for the digital redesign system. The digital redesign controller (K_d, E_d) in (10) can be rewritten as

$$K_d = H^{-1}(G - \hat{G}), \tag{11a}$$

$$E_d = H^{-1}(\stackrel{\wedge}{H}E_c), \tag{11b}$$

Since H is $m \times p$ matrix, the (K_d, E_d) in (11) can be evaluated under the two restricted conditions: the state vector dimension m must be equal to input vector dimension p, and matrix H must be nonsingular. Thus, the transformation of (K_d, E_d) in (11) is not suitable for digital redesign.

3. Modulated sine block-pulse method for digital controller

There are several methods can obtain the transformation from original continuous-time controller (K_c , E_c) to digital redesign controller (K_d, E_d) , the block-pulse function methods are often applied to get the transformation, for the well-known example block-pulse function with trapezoidal method (or bilinear transformational method), and its applying skill of block-pulse function and

assuming are as follows:

The discrete form of open-loop system in (1) can be gotten as

$$x_c(kT+T) = G x_c(kT) + \int_{kT}^{kT+T} \exp\left\{A(kT+T-\lambda)\right\} B u_c(\lambda) d\lambda$$
(12)

As a block-pulse function $\Phi_k(t)$ be applied to the continuous-time function $u_c(t)$, the $u_c(t)$ can be represented with the block-pulse function series [7] as shown in figure 2

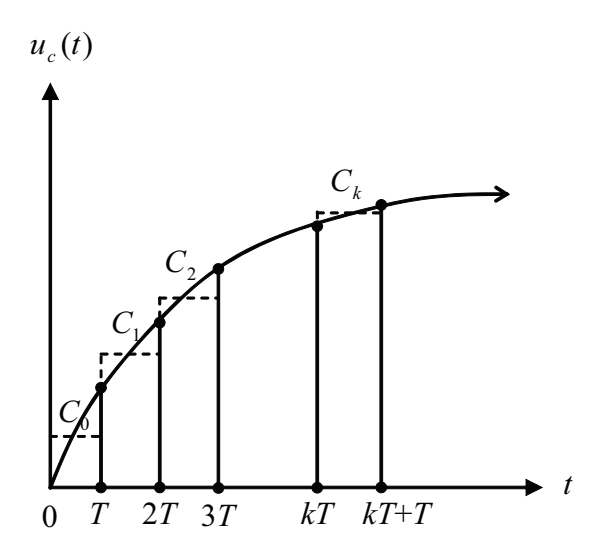


Figure 2. Applying block-pulse function series response

and described as

$$u_c(t) = \sum_{k=0}^{\infty} C_k \Phi_k(t)$$
 (13a)

Where

$$\Phi_k(t) = \begin{cases}
1 & \text{for } kT \le t < kT + T \\
0 & \text{otherwise}
\end{cases}$$
(13b)

and the equivalent weighting constant C_k can be evaluated by

$$C_{k} = \frac{1}{T} \int_{0}^{\infty} u_{c}(t) \Phi_{k}(t) dt = \frac{1}{T} \int_{kT}^{kT+T} u_{c}(t) dt \quad (13c)$$

Applying the result of (13) to (12), the discrete form of open-loop system can be

rewritten as

$$x_c(kT+T) = Gx_c(kT) + \int_{kT}^{kT+T} \exp\left\{A(kT+T-\lambda)\right\} d\lambda B \cdot C_k = Gx_c(kT) + HC_k$$

(14)

To obtained the C_k in sampling intervals, the block-pulse function with trapezoidal method assumes that the response of $u_c(t)$ in sampling intervals always form a straight line, so the integral area of $u_c(t)$ in a sampling interval will be approximately obtained as

$$\int_{kT}^{kT+T} u_c(t) dt = \frac{1}{2} T \left[u_c(kT) + u_c(kT+T) \right]$$
 (15)

Accordingly, in a continuous-time integration, if the most of the available sampled data form a straight line or a loworder curve, then applying trapezoidal method will produce a smaller error and obtain a more precise equivalent weighting constant $C_{\scriptscriptstyle k}$ in discrete processes. Consequently, the trapezoidal integration method generally achieves good performance as a smaller sampling period is used to redesign a system, because in a smaller sampling interval, the sampling data in a continuous-time integration forms a very slight curve, not so different to a straight line. Meanwhile, the trapezoidal integration method is unsuitable for systems with larger sampling periods since it will produce greater error and obtain a less precise equivalent weighting constant C_k in the discrete process. However, the actual sampled data in a continuous-time integration generally form an ark, the magnitude of which frequently varies owing to different system models and sampling periods. These arc curves obviously often resemble some part of a modulated sine function curve, since the modulated sine function significantly influences oscillation responses for stable systems.

A stable controlled system as shown in figure 1, the time-domain responses of $u_c(t)$ and $x_c(t)$ gradually converge with an oscillation form. Scanning the whole convergent oscillation response process of $u_c(t)$ and $x_c(t)$ with the viewpoint on the segmental curves reveals that the segmental responses of $u_c(t)$ and $x_c(t)$ in most sampling intervals resemble an arc curve, as displayed in figure 3a.

Consequently, the precise integral area of $u_c(t)$ in a sampling interval can be assessed by the proposed numerical integration method, as follows:

Let y(t) denote the time-domain response of a stable system. Considering the integral area of y(t) in a sampling interval given by

$$A = \int_{kT}^{kT+T} y(t) dt \tag{16}$$

Since the response factor in y(t) consists of the modulation sine function convergent exponential function, the response of y(t) is contained in a sampled interval which generally forms an arc curve, and these arc curves frequently resemble the shrinkage of a sine function curve, a modulated sine function is applied for approaching these arc curves. For figure 3a, the continuous-time integration area of an arc curve sampling interval can be derived based on the rectangular area A_1 (area abed) and the modulated sine area A_2 (area bee with dash arc). Area $A_1 = T \cdot y(kT)$ and area A_2 is assessed as follows: Let A_t denote the triangular area △ bce which is particularly considered with A_2 in figure 3b, and show a useful relation between modulated curve area A_2 and A_t . The horizontal coordinate values of points b and e are with t=0 and t=T, respectively, and let point c denote the corresponding point on a modulated sine function $\sin(nt)$ with t=T, where n is the modulated parameter. The triangular area A_t can be derived as

$$A_{t} = \frac{1}{2} \cdot \overline{\text{be}} \cdot \overline{\text{ce}} = \frac{1}{2} T \sin(nT)$$

and the modulated sine area A_2 is

$$A_2 = \int_0^T \sin(nt) dt = \frac{1}{n} [1 - \cos(nT)]$$

Moreover, the correlation of A_2 and A_t yields

$$\frac{A_2}{A_t} = \frac{2}{nT} \left[\frac{1 - \cos(nT)}{\sin(nT)} \right]$$

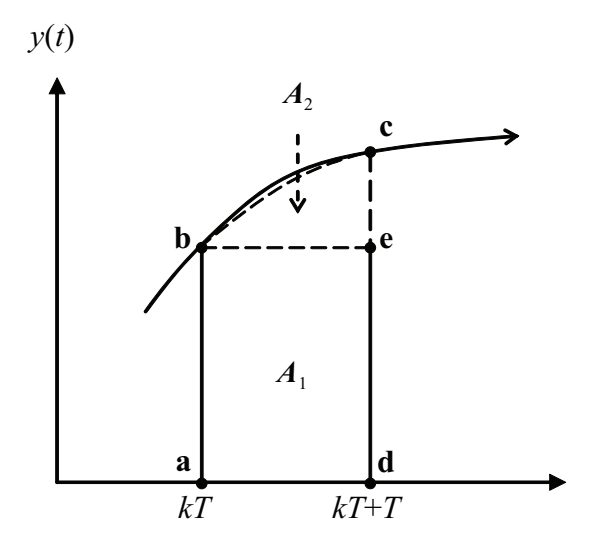


Figure 3a. A convergent block-pulse internal response

sin(nt)

Figure 3b. The modulation sine area A_2

T

or

$$A_2 = \left\lceil \frac{2}{nT} \tan \left(\frac{nT}{2} \right) \right\rceil A_{\rm t}$$

Thus, in figure 3a, the area $A_1 = \frac{1}{2}T[y(kT+T) - y(kT)] \text{ and } A_2 \text{ is}$

$$A_2 = \left[\frac{2}{nT} \tan\left(\frac{nT}{2}\right)\right] \cdot \frac{1}{2} T \left[y(kT+T) - y(kT)\right]$$
$$= \frac{1}{n} \tan\left(\frac{nT}{2}\right) \left[y(kT+T) - y(kT)\right]$$

Based on the above geometric method, equation (16) is got as

$$A = \int_{kT}^{kT+T} y(t) dt = A_1 + A_2$$

$$= \left\{ \left[1 - \frac{1}{nT} \tan\left(\frac{nT}{2}\right) \right] y(kT) + \frac{1}{nT} \tan\left(\frac{nT}{2}\right) y(kT+T) \right\} T$$
(17)

By applying the result in (17), the integral area of $u_c(t)$ in a sampling interval by proposed method will be approximately obtained as

$$\int_{kT}^{kT+T} u_c(t) dt = \left\{ \left[1 - \frac{1}{nT} \tan\left(\frac{nT}{2}\right) \right] u_c(kT) + \frac{1}{nT} \tan\left(\frac{nT}{2}\right) u_c(kT+T) \right\} T$$
(18)

and the equivalent weighting constant C_k

can be gotten by

$$C_k = \left\{ \left[1 - \frac{1}{nT} \tan\left(\frac{nT}{2}\right) \right] u_c(kT) + \frac{1}{nT} \tan\left(\frac{nT}{2}\right) u_c(kT + T) \right\}$$

(19)

Consequently, the $u_c(t)$ by the modulated sine block-pulse method can be represented as

$$u_c(t) = \sum_{k=0}^{\infty} \left\{ \left[1 - \frac{1}{nT} \tan\left(\frac{nT}{2}\right) \right] u_c(kT) + \frac{1}{nT} \tan\left(\frac{nT}{2}\right) u_c(kT+T) \right\} \Phi_k(t)$$

Substituting the result of (19) into (14), it obtains

$$x_{c}(kT+T) = Gx_{c}(kT) + H\left\{ \left[1 - \frac{1}{nT} \tan\left(\frac{nT}{2}\right) \right] u_{c}(kT) + \frac{1}{nT} \tan\left(\frac{nT}{2}\right) u_{c}(kT+T) \right\}$$

$$(21)$$

The continuous-time state-feedback control laws $u_c(t) = -K_c x_c(t) + E_c r(t)$ at sampling time kT and kT + T are substituted into (21), namely

$$\begin{split} x_c(kT+T) = &\left\{G - \left[1 - \frac{1}{nT}\tan\left(\frac{nT}{2}\right)\right]HK_c\right\}x_c(kT) - \frac{1}{nT}\tan\left(\frac{nT}{2}\right)HK_cx_c(kT+T) \right. \\ &\left. + \left[1 - \frac{1}{nT}\tan\left(\frac{nT}{2}\right)\right]HE_cr(kT) + \frac{1}{nT}\tan\left(\frac{nT}{2}\right)HE_cr(kT+T) \right. \end{split}$$

(22)

Assuming a step input is used (r(kT) = r(kT + T)) and rearranging (22), it yields

$$\begin{split} x_c(kT+T) = & \left[I_m + \frac{1}{nT}\tan\left(\frac{nT}{2}\right)HK_c\right]^{-1}\left\{G - \left[1 - \frac{1}{nT}\tan\left(\frac{nT}{2}\right)\right]HK_c\right\}x_c(kT) \\ + & \left[I_m + \frac{1}{nT}\tan\left(\frac{nT}{2}\right)HK_c\right]^{-1}HE_cr(kT) \end{split}$$

(23)

The above result in (23) is the designed continuous-time equation at the sampling instant. The comparison of (23) and the corresponding redesigned discrete-time model in (8) is given as

$$G - HK_d = \left[I_m + \frac{1}{nT} \tan\left(\frac{nT}{2}\right) HK_c\right]^{-1} \left\{G - \left[1 - \frac{1}{nT} \tan\left(\frac{nT}{2}\right)\right] HK_c\right\}$$
(24a)

$$HE_d = \left[I_m + \frac{1}{nT} \tan\left(\frac{nT}{2}\right) HK_c\right]^{-1} HE_c \qquad (24b)$$

From (24), the digitally redesigned feedback gain K_d and forward gain E_d are reduced to

$$K_{d} = \left[I_{p} + \frac{1}{nT}\tan\left(\frac{nT}{2}\right)K_{c}H\right]^{-1}K_{c}\left\{\left[1 - \frac{1}{nT}\tan\left(\frac{nT}{2}\right)\right]I_{m} + \frac{1}{nT}\tan\left(\frac{nT}{2}\right)G\right\}$$
(25a)

$$E_d = \left[I_p + \frac{1}{nT} \tan\left(\frac{nT}{2}\right) K_c H \right]^{-1} E_c$$
 (25b)

From the designed continuous-time model, A, B, K_c and E_c are known, and G and H are given from (9c) and (9d), thus the redesigned discrete-time gains K_d and E_d can be obtained from (25), and the system responses of the digitally redesigned system will closely match that of the originally continuous-time system.

On the other systematic approaches, the digitally redesigned gains proposed in this paper have some relation to those via improved block-pulse function method [4] and block-pulse function with trapezoidal method [3]. For comparison, different superscripts are added on controller gains to designate each associated method as follows:

(i)Improved block-pulse function method
[4]

$$K_d^+ = \frac{1}{T} K_c \hat{A}^{-1} (\hat{G} - I_m)$$
 (26a)

$$E_{d}^{+} = [I_{p} + K_{c} \hat{A}^{-1} (B - \frac{1}{T} \hat{H})] E_{c}$$
 (26b)

where $\hat{A} = A - BK_c$, $\hat{G} = \exp\{(A - BK_c)T\}$ and

$$\stackrel{\wedge}{H} = (\stackrel{\wedge}{G} - I_{m}) \stackrel{\wedge}{A}^{-1} B.$$

(ii)Block-pulse function with trapezoidal method [3]

$$K_d^* = \frac{1}{2} (I_p + \frac{1}{2} K_c H)^{-1} K_c (I_m + G)$$
 (27a)

$$E_d^* = (I_p + \frac{1}{2}K_cH)^{-1}E_c$$
 (27b)

where $G = \exp(AT)$ and $H = (G - I_m)A^{-1}B$.

(iii) The proposed method that the results of K_d and E_d are shown in (25a) and (25b).

4. Illustrative example

Consider a continuous-time designed system [3,4,8]

$$\dot{x}_c(t) = Ax_c(t) + Bu_c(t), x_c(0) = \begin{bmatrix} 0 & 0 & 0 & 0 \end{bmatrix}'$$

with the designed controller

$$u_c(t) = -K_c x_c(t) + E_c r(t)$$

where

$$A = \begin{bmatrix} 0.809 & -2.060 & 0.325 & 0.465 & 0.895 \\ 6.667 & 0.200 & 1.333 & 0.000 & 0.667 \\ -1.291 & 0.458 & -1.072 & -2.326 & -0.199 \\ -0.324 & 0.824 & 1.670 & -1.186 & -0.358 \\ -3.509 & -4.316 & -0.702 & 0.000 & -8.351 \end{bmatrix}$$

$$B = \begin{bmatrix} 0.955 & -0.379 \\ -1.667 & -1.667 \\ -0.212 & 1.195 \\ 0.618 & 0.052 \\ 0.877 & 1.403 \end{bmatrix}$$

$$K_c = \begin{bmatrix} 7.871 & -0.563 & 3.255 & -0.137 & 0.754 \\ 1.625 & -1.247 & 1.297 & -1.003 & 0.182 \end{bmatrix}$$

$$E_c = \begin{bmatrix} 1.0 & 0.0 \\ 0.0 & 1.0 \end{bmatrix}$$

It is desired to find an equivalent digital control law $u_d(t) = -K_d x_d(kT) + E_d r(kT)$ such that $x_d(kT)$ in (8) can match $x_c(t)\Big|_{t=kT}$ in

(3) with the piecewise-constant control input $u_d(t) = u_d(kT)$ for $kT \le t < kT + T$.

For fair comparison, the sampled-data performance indices are proposed and respectively defined as follows:

$$J_{X_n} = \int_0^{t_f} \left| x_{nc}(t) - x_{nd}(t) \right| dt$$

$$\equiv \sum_{k=0}^{t_f} \sum_{h=0}^{h_f-1} \left\{ \left| x_{nc}(t = kT + h \cdot \frac{T}{h_f}) - x_{nd}(t = kT + h \cdot \frac{T}{h_f}) \right| \cdot \frac{T}{h_f} \right\}$$

and

$$J_S = \sum_{n=1}^5 J_{\chi_n}$$

where J_{x_n} are the state response errors of $x_1 \sim x_5$ for time response from 0 to t_f second between continuous-time system and the digital redesign system,

$$k_f = \operatorname{int}\left(\frac{t_f}{T}\right)$$
 is the final sampling point

during the whole response section, and h_f is the number of evaluated points during one sampling interval. The J_s is the summation of state response errors of the digital redesign system.

For clear comparison, we compute the state summation error J_s ($t_f = 7$ sec and $h_f = 100$ are chosen) via the three digital redesign methods at different sampling period, and those evaluations of J_s are shown in figure 4.

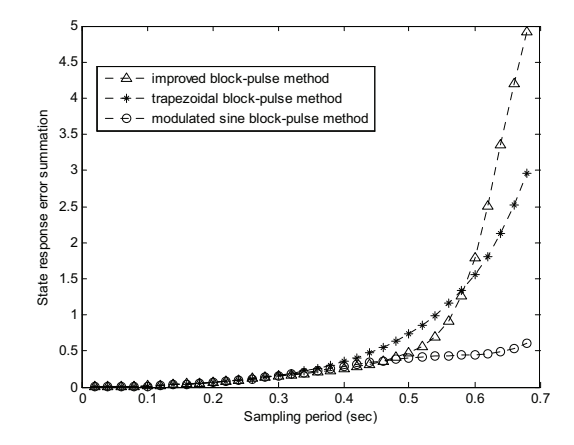


Figure 4. J_s of three methods in different sampling periods

It is seen that there are 34 different sampling periods ($T = 0.02, 0.04, 0.06, \dots, 0.68$) are chosen to compute these J_S of three

methods. In order to look for the optimum modulated parameter n of the proposed method using the illustrated example, the sum of J_S ($t_f=7$ sec, $h_f=100$) of proposed method using different modulated parameter n at 34 different sampling periods is calculated and shown in figure 5.

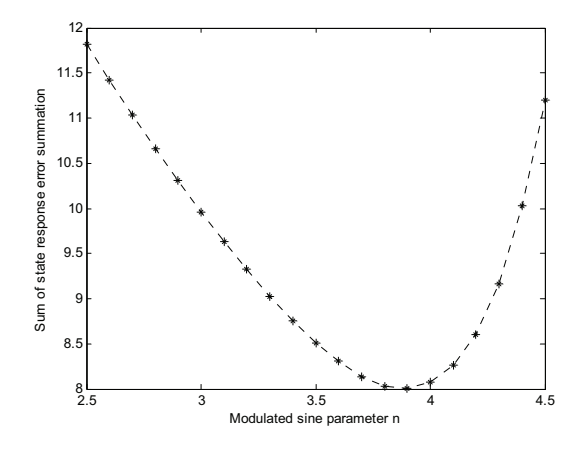


Figure 5. The sum of J_S of proposed method using different modulated sine parameter n

Clearly, the n=3.9 has the least error, thus it also is the most suitable modulated parameter value of proposed method for redesigning the illustrated system. In figure 4, n=3.9 is used in proposed method to compare with other two methods, and there are some phenomena are found as follows:

As sampling period T < 0.3 sec, the J_s of digital redesign system via the three methods are close, so the three digital redesign methods have similar good performance in this sampling interval.

As 0.3 < T < 0.5 sec, the two performance indices J_S with (K_d^+, E_d^+) and (K_d^-, E_d^-) are less than J_S^- with (K_d^*, E_d^*) . So the improved block-pulse method and modulated sine block-pulse method have

similar better performance than trapezoidal block-pulse method in this sampling interval.

As 0.5 < T < 0.58 sec, the performance index J_S with (K_d^+, E_d^+) is less than the J_S with (K_d^*, E_d^*) , and the J_S with $(K_d E_d)$ is the least among the three method. In this sampling interval, the modulated sine block-pulse method has the best performance, the improved block-pulse method is the second and trapezoidal block-pulse method is the last.

As T > 0.58 sec, the performance index J_s with (K_d^+, E_d^+) is greater than the J_s with (K_d^*, E_d^*) , and the J_s with $(K_d E_d)$ is also the comparatively least among the three method. Thus, in this sampling interval, the modulated sine block-pulse method has the best performance, the trapezoidal block-pulse method is the second and improved block-pulse method is the last.

The conclusion in above discussion is tabulated in table 1 for comparison. In this example, the proposed method has superior performance display at most of selected sampling periods.

Then let us choose two sampling periods to verify the above conclusion. First, a sampling period T = 0.25 sec is selected for the discrete-time model. The digitally redesigned gains in (26) via the improved block-pulse function method are given by

$$K_d^+ = \begin{bmatrix} 1.9829 & -0.8894 & 0.7346 & 0.0414 & 0.1887 \\ -0.6402 & -0.8736 & 0.1619 & -0.7175 & -0.0407 \end{bmatrix}$$

$$E_d^+ = \begin{bmatrix} 0.4057 & -0.2801 \\ -0.1163 & 0.7240 \end{bmatrix}$$

By utilizing the trapezoidal block-pulse method, the desired gains in (27) are

$$K_d^* = \begin{bmatrix} 2.6260 & -0.7954 & 1.0335 & 0.0346 & 0.2494 \\ -0.3370 & -0.8712 & 0.3071 & -0.7327 & -0.0117 \end{bmatrix}$$

$$E_d^* = \begin{bmatrix} 0.4772 & -0.2532 \\ -0.0903 & 0.7476 \end{bmatrix}$$

Also, the gains in (25) via modulated sine block-pulse method with n=3.9 are

$$K_{\scriptscriptstyle d} = \begin{bmatrix} 2.4598 & -0.8132 & 0.9667 & 0.0354 & 0.2335 \\ -0.4208 & -0.8452 & 0.2614 & -0.7168 & -0.0201 \end{bmatrix}$$

$$E_d = \begin{bmatrix} 0.4582 & -0.2576 \\ -0.0919 & 0.7334 \end{bmatrix}$$

Choosing $t_f = 2.5$ sec, the state responses of $x_1 \sim x_5$ of the continuous-time system and digital redesigned system with (K_d^+, E_d^+) , (K_d^*, E_d^*) and $(K_d E_d)$ are together shown in figure 6, and the evaluations of the performance indices are tabulated in table 2 for comparison. In this example, each simulated performance index of $J_{x_1} \sim J_{x_5}$ is numerically evaluated via 100 points $(h_f = 100)$ during one sampling interval.

Second, a sampling period T=0.64 sec and $t_f=7$ sec are chosen for the discrete-time model, and the state responses of the continuous-time system and digital redesigned system with (K_d^+, E_d^+) , (K_d^*, E_d^+) and $(K_d E_d)$ are shown in figure 7a, figure 7b and figure 7c, respectively. Moreover, the all evaluations of the performance indices of the state response in figure 7 are tabulated in table 3 for comparison.

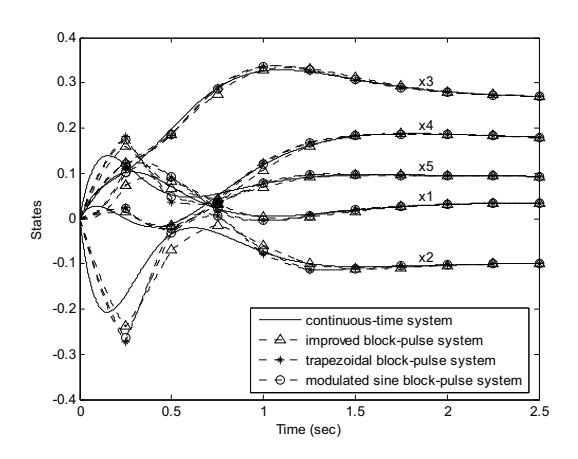


Figure 6. The states responses of three redesigned method with T=0.25(sec)

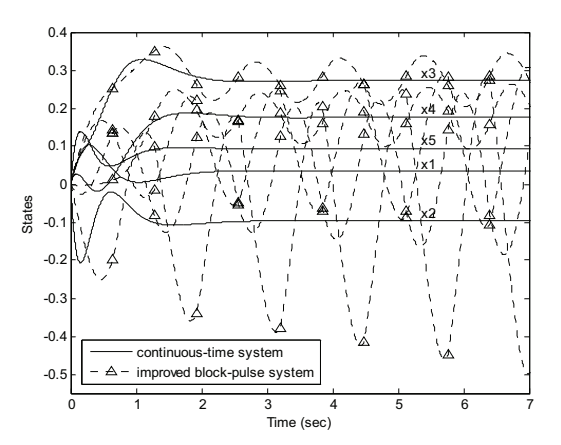


Figure 7a. Improved block-pulse method with T=0.64(sec)

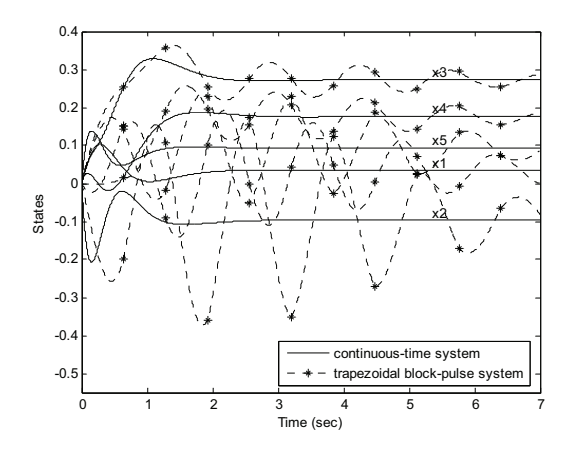


Figure 7b. Bilinear transformation method with T=0.64(sec)

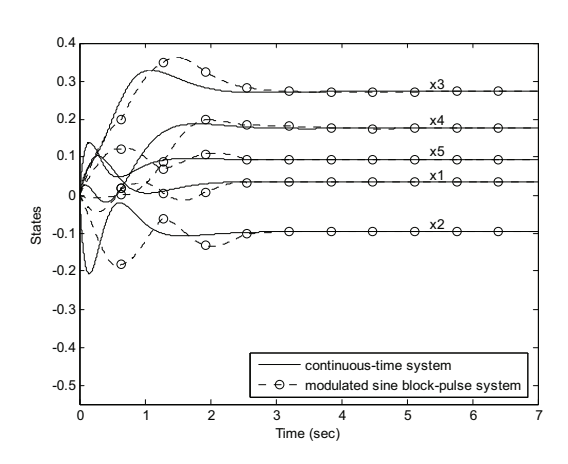


Figure 7c. Modulated sine method with T=0.64 (sec)

From figure 6 and table 2, as sampling period is not great, it is shown that the digital redesigned state responses of three methods are similar, and they have closely good performance display. It is interested increase the sampling period Tgradually, as T = 0.64 sec, the digital responses via improved block-pulse method are divergent as shown in figure 7a, but the responses via trapezoidal block-pulse method and via proposed method with n=3.9 are still convergent as shown in figure 7b and figure 7c, respectively, and proposed method has a fewer state response error.

Figures 6-7 and tables 1-3 reveal that digital redesign controlled system via the proposed method with a suitable *n* display good performance in discrete-time response and tolerate a wider sampling period for sample-data implementation.

5. Conclusion

A new method for digital redesign of an analog controller for a sampled-data system has been presented. Because the proposed method is fitter for the actual response curves of a stable system, it can be more effective in digitalizing an implemented analog system. The proposed method. modulated sine block-pulse method, adjustable function has a parameter, the user can suitably chosen the value of the modulation parameter depending on the defined cost function with a least discretized error sum for a system. Consequently, via control beforehand simulation, when a suitable modulated parameter value in the proposed method is utilized to digitalize an analogue controlled system, not only the resulting dynamic states of the digital redesign controlled sampled-data system are able to closely match those of the original controlled continuous-time system, but also the new digitally redesigned system can tolerate a larger sampling period when compared to other redesign methods.

The proposed digital redesign method is more advantageous to the cases in which the sampling rates are relatively slow due to the hardware constraints or the transient responses are especially emphasized. Throughout the proposed method disclosed in this paper, a more precise digital redesigned system can be obtained.

6. Reference

- 1 K. Ogata, Discrete-time Control System, Prentice-Hall, Englewood Cliffs, N. J., 1987.
- 2 C.T. Chen, Analog and Digital Control System Design: Transfer-function, Statespace, and Algebraic Methods, Saunders College Publishing, Orlando, 1993.
- 3 J.S.H Tsai, L.S. Shieh, J.L. Zhang and N.P. Coleman, Digital Redesign of Pseudo-Continuous-Time Suboptimal

- Regulators for Large-Scale Discrete Systems, Control-Theory and Advanced Technology (C-TAT) Vol. 5 No.1 (1989) 37-65.
- 4 J.S.H. Tsai, L.S. Shieh and J.L. Zhang, An Improvement of the Digital Redesign Method Based on the Block-Pulse Function Approximation, Circuits, Systems and Signal Processing Vol. 12 No. 1 (1993) 37-49.
- 5 L.S. Shieh, X.M. Zhao and J.L. Zhang, Locally Optimal-Digital Redesign of Continuous-Time System, IEEE Trans. Industrial Electronics Vol. 36 No. 4 (1989) 511-515.

- 6 L.S. Shieh, H. Wang and R.E. Yates, Discrete-Continuous Model Conversion, Applied Math. Modeling Vol. 4 No. 6 (1980) 449-455.
- 7 L.S. Shieh, C.K. Yeung and B.C. Mcinnis, Solution of the State-Space Equations via Block-Pulse Function, International Journal of Control Vol. 28 No. 3 (1978) 383-392.
- 8 L.S. Shieh, J.L. Zhang and S. Ganesan, Pseudo-Continuous-Time Quadratic Regulators with Pole Placement in a Specific Region, IEE Proceeding D. Control Theory & Applications Vol. 137 No. 5 (1990) 338-346.

Table 1. The performance order of three methods in different sampling time interval

					8
Performance order 0		0 < T < 0.3	0.3 < T < 0.5	0.5 < T < 0.58	0.58 < T
	K_d^+ , E_d^+	①	①	2	3
	K_d^* , E_d^*	①	2	3	2
	K_d , E_d	①	①	①	①

Table 2. Error comparison with the sampling period T=0.25(sec)

	$J_{\chi_{_{ m l}}}$	J_{x_2}	J_{χ_3}	J_{χ_4}	J_{χ_5}	$J_{\scriptscriptstyle S}$
K_d^+ , E_d^+	0.0207	0.0399	0.0131	0.0137	0.0213	0.1088
K_d^* , E_d^*	0.0199	0.0404	0.0108	0.0114	0.0226	0.1050
K_d , E_d	0.0196	0.0391	0.0105	0.0112	0.0218	0.1021

Table 3. Error comparison with the sampling period T=0.64(sec)

	J_{x_1}	J_{χ_2}	J_{χ_3}	J_{χ_4}	J_{χ_5}	$J_{\scriptscriptstyle S}$
K_d^+ , E_d^+	0.7787	1.3178	0.2521	0.3052	0.7063	3.3602
K_d^* , E_d^*	0.4899	0.8228	0.1717	0.2077	0.4358	2.1279
K_d , E_d	0.0972	0.1475	0.0824	0.0870	0.0753	0.4894